TFEB-mediated autophagy rescues midbrain dopamine neurons from α-synuclein toxicity

Mickael Decressac[a,1], Bengt Mattsson[a], Pia Weikop[b], Martin Lundblad[a], Johan Jakobsson[a], and Anders Björklund[a,1]

[a]Department of Experimental Medical Sciences, Wallenberg Neuroscience Center, Lund University, 22184 Lund, Sweden; and [b]Laboratory of Neuropsychiatry, Rigshospitalet University Hospital, DK-2100 Copenhagen, Denmark

Contributed by Anders Björklund, March 26, 2013 (sent for review November 22, 2012)

The aggregation of α-synuclein plays a major role in Parkinson disease (PD) pathogenesis. Recent evidence suggests that defects in the autophagy-mediated clearance of α-synuclein contribute to the progressive loss of nigral dopamine neurons. Using an in vivo model of α-synuclein toxicity, we show that the PD-like neurodegenerative changes induced by excess cellular levels of α-synuclein in nigral dopamine neurons are closely linked to a progressive decline in markers of lysosome function, accompanied by cytoplasmic retention of transcription factor EB (TFEB), a major transcriptional regulator of the autophagy-lysosome pathway. The changes in lysosomal function, observed in the rat model as well as in human PD midbrain, were reversed by overexpression of TFEB, which afforded robust neuroprotection via the clearance of α-synuclein oligomers, and were aggravated by microRNA-128–mediated repression of TFEB in both A9 and A10 dopamine neurons. Delayed activation of TFEB function through inhibition of mammalian target of rapamycin blocked α-synuclein induced neurodegeneration and further disease progression. The results provide a mechanistic link between α-synuclein toxicity and impaired TFEB function, and highlight TFEB as a key player in the induction of α-synuclein–induced toxicity and PD pathogenesis, thus identifying TFEB as a promising target for therapies aimed at neuroprotection and disease modification in PD.

adeno-associated virus | Beclin | aggregates | synucleinopathy

A major hallmark of Parkinson disease (PD) that contributes to the progressive loss of nigral dopamine (DA) neurons is α-synucleinopathy. Defects in clearance of oligomeric or misfolded proteins have been associated with aging and several neurodegenerative disorders (1–4). In human PD and related Lewy Body diseases, the presence of α-synuclein–positive (α-syn$^+$) aggregates is associated with accumulation of autophagosomes and reduction of lysosomal markers in affected nigral DA neurons, suggesting a defect in lysosome-mediated clearance of α-syn aggregates (5–7).

How dysfunction of the autophagy-lysosome pathway (ALP) contributes to the pathogenesis of PD remains unclear. Under physiological conditions, α-syn is degraded by the ubiquitin-proteasome system and the ALP, including macroautophagy and chaperone-mediated autophagy (6, 8–12). In cases of α-syn overload, however, misfolded or mutated α-syn fails to be processed and α-syn clearance by chaperone-mediated autophagy is blocked (12–15). In this situation, processing of excess α-syn, or toxic α-syn species, will depend on the functional integrity of the macroautophagy pathway (14). In support, it has been shown that mice deficient in one of the autophagy-related (atg) proteins develop neurodegeneration, and that deficiency in atg7 or the PD-associated protein PARK9 (ATP13A2, a lysosomal ATPase) causes PD-like neurodegeneration, both in vitro and in vivo (7, 16–19). In humans, PD has been genetically linked to the rare lysosomal storage diseases, Gaucher disease and Sanfilippo syndrome (20, 21), and polymorphism in the lysosomal genes Lysosomal associated membrabe protein 2 (LAMP2) and Adenosine-3-phosphate 13A2 (ATP13A2) has recently been linked with PD (22, 23).

The role of autophagy in the elimination of toxic protein species has generated interest in the development of therapeutic strategies for neurological diseases characterized by protein misfolding and aggregation (4, 24, 25). Genetic strategies based on overexpression of an ALP activator, Beclin-1, have been shown to be effective in reducing protein aggregation and pathology in cellular and animal models (26–28), and pharmacological activation of ALP function by inhibition of the mammalian target of rapamycin (mTOR) has produced similar protective effects in animal models of PD and other neurodegenerative diseases (6, 7, 29–34).

Recently, Ballabio and colleagues identified the transcription factor EB (TFEB) as a master regulator of the ALP (35, 36), controlled by mTOR signaling (37–39). Enhancement of TFEB function has been shown to stimulate ALP function and promote protein clearance and neuroprotection in cellular models of protein misfolding and oxidative stress, as well as in a mouse model of Huntington disease (7, 35, 40). Here, we provide evidence that mechanistically links α-syn–mediated toxicity to impaired TFEB function both in a rodent PD model and in human PD. We have used an in vivo model of α-syn toxicity and report that TFEB function, as reflected by its translocation to the nucleus, is impaired in α-syn overexpressing midbrain DA neurons, and that the reduced nuclear expression of TFEB is seen also in midbrain DA neurons in human PD. This impairment was associated with a progressive decline in markers of lysosome function, accumulation of α-syn oligomers, and development of DA neuron pathology and cell death. These degenerative changes are efficiently blocked by overexpression of TFEB, resulting in almost complete protection of nigral DA neurons and elimination of

Significance

This study shows that neurodegenerative changes induced by α-synuclein in midbrain dopamine neurons in vivo can be blocked through activation of the autophagy-lysosome pathway. Using an adeno-associated virus model of Parkinson disease to overexpress α-synuclein in the substantia nigra, we show that genetic [transcription factor EB (TFEB) and Beclin-1 overexpression] or pharmacological (rapalog) manipulations that enhance autophagy protect nigral neurons from α-synuclein toxicity, but inhibiting autophagy exacerbates α-synuclein toxicity. The results provide a mechanistic link between α-synuclein toxicity and impaired TFEB function, and identify TFEB as a target for therapies aimed at neuroprotection and disease modification in Parkinson disease.

Author contributions: M.D. and A.B. designed research; M.D., B.M., P.W., and M.L. performed research; J.J. contributed new reagents/analytic tools; M.D. and A.B. analyzed data; M.D. and A.B. wrote the paper; P.W. performed the HPLC analyses; M.L. performed the amperometry measurements and analyzed these data; and J.J. designed the microRNA vector.

The authors declare no conflict of interest.

[1]To whom correspondence may be addressed. E-mail: Mickael.Decressac@med.lu.se or anders.bjorklund@med.lu.se.

This article contains supporting information online at www.pnas.org/lookup/suppl/doi:10.1073/pnas.1305623110/-/DCSupplemental.

α-syn oligomers, and that repression of TFEB by microRNA-128 (miR-128) exacerbated the vulnerability to α-syn toxicity in both A9 and A10 DA neurons. Finally, we show that delayed pharmacological activation of TFEB function, through inhibition of mTOR, is highly efficient in blocking α-syn–induced degenerative changes and further disease progression in the affected DA neurons. Taken together, these data provide evidence for a central role of TFEB in the cellular defense against α-syn toxicity and as a key player in PD pathogenesis.

Results

α-Synuclein Overexpression Causes Dynamic Changes in the ALP in DA Neurons. Adeno-associated virus (AAV) vector-mediated overexpression of human wild-type α-syn in the rat midbrain, resulting in a three- to fourfold increase in α-syn mRNA (41), has previously been shown to induce PD-like neuropathology in nigral DA neurons, including accumulation of α-syn inclusions and progressive development of degenerative changes in axons and cell bodies that replicate both presymptomatic and advanced stages as seen in the human condition (41–43). To what extent these changes reflect alterations in ALP processing, however, is so far not known. In the present study we have monitored changes in ALP function in the AAV–α-syn model using markers of autophagic and lysosomal activity. At the presymptomatic stage (10 d after vector injection), when α-syn is well expressed and α-synucleinopathy is developing but before any cell death has occurred (Fig. S1)—the mRNA and protein expression of autophagic (Beclin-1, LC3I/II) and lysosomal (Lamp-1, Cathepsin B and D) markers was significantly increased (protein level of Beclin-1: +188%; LC3II: +367%; Lamp-1: +114%; Cathepsin D: +138%; $P < 0.01$ compared with GFP group: $n = 5$ per group); the TFEB level remained unchanged (Fig. 1 *A* and *B*). Between 10 d and 3 wk, when cell loss starts to occur (Fig. 1*B* and Fig. S1), mRNA levels of ALP markers started to decline (Fig. 1*A*) and Western blot analysis revealed a sustained increase in the expression of autophagic markers (Beclin-1: +74%, LC3: +58%, $P < 0.05$; $n = 5$ per group), suggesting an accumulation of autophagosomes; a lysosomal depletion was assessed by the reduced levels of Lamp-1 (−11%) and Cathepsin D (−33%) ($P > 0.05$ compared with GFP group; $n = 5$ per group) (Fig. 1*B*).

Histological analysis revealed that aggregated human α-syn colocalized with Beclin-1, Cathepsin D, and the cargo receptor p62 in DA neurons (Fig. 1 *C–E*). Impaired α-syn clearance by the ALP was also seen at the symptomatic stage (8 wk) (Fig. S1), because surviving cells overexpressing α-syn showed ubiquitin-positive aggregated material and increased levels of p62 (by 3.1 ±

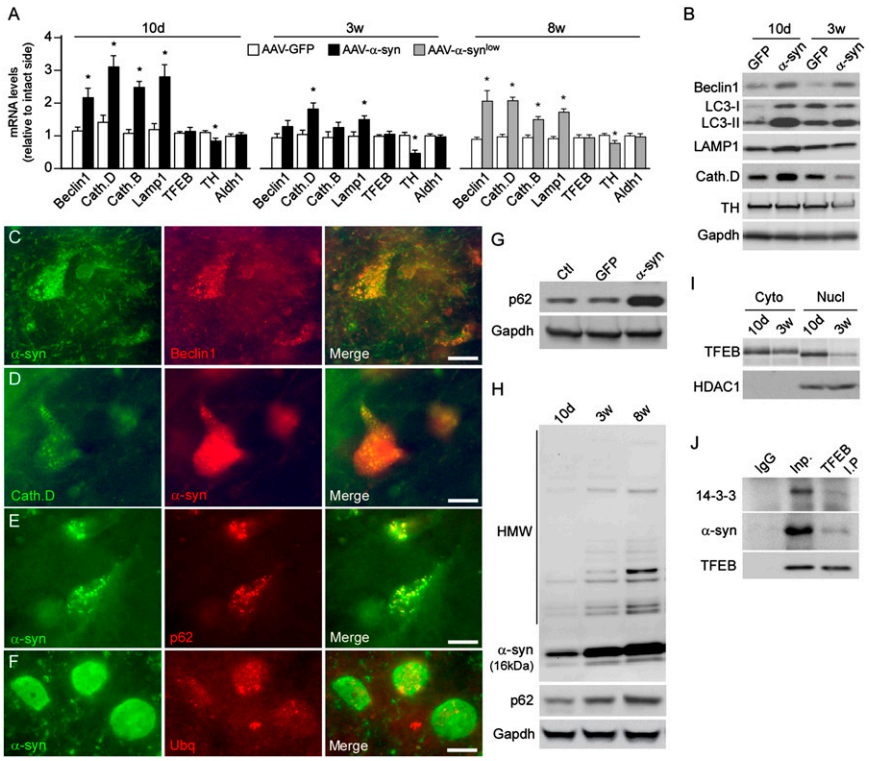

Fig. 1. α-Synuclein impairs autophagy by sequestrating TFEB. (*A*) qPCR analysis showing mRNA expression of ALP markers (Beclin-1, Cathepsin B, Cathepsin D, Lamp-1, and TFEB) and dopaminergic markers (TH and Aldh1) in the ventral midbrain 10 d, 3 wk, and 8 wk after intranigral injection of AAV-GFP (white bar) or AAV–α-syn vectors at high (2.1×10^{12} gc/mL) (black bar) and low concentration (3.8×10^{11} gc/mL) (gray bar). *$P < 0.05$ compared with AAV-GFP group (Student *t* test) ($n = 5$ per group). (*B*) Protein expression of Beclin-1, Lamp-1, Cathepsin D, LC3I/II, and TH in the midbrain 10 d (presymptomatic stage), and 3 wk (initiation of neurodegeneration) after overexpression of GFP or α-syn. (*C–E*) Fluorescent immunohistochemistry showing the colocalization of human α-syn with Beclin-1 (*C*), Cathepsin D (*D*), and p62 (*E*) 3 wk after intranigral injection of AAV–α-syn. (Scale bars, 15 μm.) (*F*) Fluorescent immunohistochemistry illustrating the accumulation of dense ubiquitin-positive structures inside DA neurons overexpressing α-syn 8 wk after AAV–α-syn injection. (Scale bar, 15 μm.) (*G*) Western blot showed an important accumulation of the autophagy substrate p62 8 wk after AAV–α-syn injection in the SN compared with the GFP and control group. (*H*) Western blot analysis illustrating the progressive accumulation of high molecular weight (HMW) α-syn oligomers in the striatum and p62 in midbrain extracts at 10 d, 3 wk, and 8 wk after AAV–α-syn injection (high titer). (*I*) Western blot analysis showed an increased nuclear expression of TFEB at 10 d, and a reduced nuclear localization of TFEB at 3 wk after AAV–α-syn injection at high titer. Shift in the molecular weight corresponds to the phosphorylated and dephosphorylated forms of TFEB in the cytoplasm and nucleus, respectively. Control of nuclear extraction was performed by analysis of the nuclear marker HDAC1. (*J*) Coimmunoprecipitation (IP) of TFEB with α-syn and 14-3-3 in α-syn–overexpressing midbrain tissue (3 wk postinjection). Lysates were subjected to IP for TFEB or control IgG, and immunoblotted for α-syn and 14-3-3 (Inp: input, no I.P).

0.6-fold, $P < 0.01$ compared with GFP group) (Fig. 1 *F* and *G*), suggesting a failure in protein and autophagosome clearance. Western blot analysis showed that failure of the ALP was associated with a progressive accumulation of α-syn oligomers that was previously shown to be toxic for nigral neurons (44) and the autophagy substrate p62 (16, 45) (Fig. 1*H*).

When nigral neurons were transduced with a lower number of viral genome copies [about six-times fewer viral particles, 3.8×10^{11} genome copy (gc)/mL, compared with high titer, 2.1×10^{12} gc/mL, resulting in a twofold increase of α-syn mRNA (41)] (*Materials and Methods*), resulting in no or very limited cell death (Fig. S1) (42), the compensatory ALP response was still maintained 8 wk after injection (Fig. 1*A*).

Next we investigated to what extent changes in the subcellular localization of the TFEB correlated with these dynamic changes in the ALP response. Interestingly, the early response to α-syn overexpression (at 10 d) appeared to be associated with TFEB translocation into the nucleus, whereas at a later stage (3 wk), deficiency in autophagy was linked to a reduced expression in the nuclear fraction (Fig. 1*I*). Recent studies have shown that mTOR-mediated phosphorylation of TFEB leads to its sequestration by 14-3-3 proteins in the cytoplasmic compartment (38, 39). Because α-syn shares structural and functional homology with 14-3-3 proteins and can bind similar targets (46, 47), we hypothesized that they may interact with TFEB. Strikingly, coimmunoprecipitation experiments showed that both human wild-type α-syn and 14-3-3 were able to bind to TFEB (Fig. 1*J*), suggesting that α-syn overexpression may contribute to sequestration of the transcription factor into the cytoplasm, thus hampering the ALP response and, thereby, its own clearance.

Changes in TFEB Subcellular Localization in PD. To further validate our observation made in the rat model, we studied possible changes in TFEB expression in postmortem human brains. Histological examination of postmortem control brains showed that TFEB is expressed by nigral DA neurons (Fig. 2*A*) and that it distributes both in the cytoplasmic and nuclear compartments (Fig. 2*B*). Notably, observation of postmortem PD midbrains revealed a significant reduction of TFEB expression in the nuclear compartment (arrowhead in Fig. 2*E*). Furthermore, in line with our finding from the AAV rat model, TFEB colocalized with α-syn in Lewy bodies containing nigral neurons (arrow in Fig. 2*E*). In contrast, analysis of TFEB expression in ventral tegmental area (VTA) neurons revealed that its subcellular localization was not changed between control and PD human brains (Fig. 2 *F*–*H*).

Stimulation of Autophagy by TFEB Overexpression Affords Protection Against α-Syn–Induced Toxicity. These observations led us to postulate that strategies aimed at maintaining increased ALP activity may provide protection against α-syn toxicity. We first tested whether a gene-therapy approach, based on the overexpression of TFEB, could enhance ALP activity and protect nigral DA neurons in the AAV–α-syn model. For comparison, we used an AAV vector to overexpress the ALP activator Beclin-1, which has been shown previously to be effective in reducing protein aggregation in α-syn transgenic mice (26–28). AAV-TFEB and AAV–Beclin-1, delivered unilaterally over the substantia nigra (SN), resulted in increased expression of the proteins in the vast majority of nigral DA neurons. This process did not affect survival of nigral DA neurons (Fig. S2 *A*–*C*) but promoted sustained stimulation of the ALP as assessed by the increased levels of several lysosomal markers (Cathepsin B and D, Lamp-1, and LC3) (Fig. S2*D*). In TFEB-overexpressing animals, this effect was associated with nuclear expression of the transcription factor in nigral DA neurons (Fig. S2*E*). Notably, we found that, when overexpressed together with human α-syn (Fig. S2 *F* and *G*), TFEB—as well as Beclin-1—prevented the development of behavioral impairment in both spontaneous and drug-induced motor tests (Fig. 3 *A*–*C*). Histological and biochemical analysis revealed a robust and long-term protection of nigral DA neurons and striatal terminals, as well as maintenance of the striatal DA content (Fig. 3 *D*–*H*). In vivo real-time chronoamperometry measurements showed that synaptic function was also preserved (Fig. 3 *I* and *J*). Computer-based quantification of α-syn$^+$ axonal swellings and Western blot analysis of α-syn expression showed that the neuroprotective effect of TFEB and Beclin-1 most likely resulted from the reduced formation of α-syn oligomers and increased processing of autophagosomes, as indicated by a marked reduction in the accumulation of p62 (around −65% in both groups compared with α-syn+GFP group, $n = 5$, $P < 0.01$) (Fig. 3 *K*–*M*).

Effect of miR-128–Mediated Down-Regulation of TFEB in DA Neurons. Transgenic approaches have shown that deficiency in key autophagic markers is sufficient to provoke neurodegeneration of nigral DA neurons (16–19, 48). Here, we examined the effect of miR-based repression of autophagy on α-syn aggregation and toxicity. Repression of the ALP was obtained by inhibiting TFEB using AAV-mediated overexpression of miR-128, which has previously been characterized to target TFEB (35), in the rat midbrain (Fig. S3 *A* and *B*). This strategy induced a significant down-regulation in the expression of TFEB, its ALP-related targets (−20 to 40%, $P < 0.05$) (Fig. 4*A*), without affecting the expression of DA-related markers (Fig. 4*A*). Notably, nigral injection of AAV–miR-128 at a low titer did not cause a significant loss, but a higher dose induced significant degeneration of A9 neurons after 8 wk compared with an injection of the titer-matched AAV-GFP control vector (Fig. S3 *C* and *D*). When individually nontoxic doses of AAV–α-syn (Fig. S1) and AAV–miR-128 (Fig. S3) were injected as a mixed solution over the rat SN (Fig. 4 *B* and *C*), we found that miR-128 exacerbated the toxicity of α-syn, as revealed by a significant loss of nigral DA neurons, striatal innervation, and DA levels (Fig. 4 *G*–*J*) and the development of motor deficits (Fig. 4 *D*–*F*), as observed 8 wk after vector injection. MiR-128–mediated repression of TFEB led to increased formation of α-syn oligomers (Fig. 4*K*) and a marked increase in α-syn$^+$ axonal swellings (Fig. 4*L*).

Consistent with observations in postmortem PD brain tissue (49, 50), it has been shown that the A10 neurons of the VTA are less affected by AAV-mediated α-syn overexpression than the A9 nigral neurons (51). We hypothesized that more efficient protein clearance by the ALP may confer a unique resistance to this subpopulation of DA midbrain neurons against α-syn–induced toxicity. Quantitative PCR (qPCR) analysis showed that basal levels of ALP markers was not different between neurons from the medial (VTA) and lateral (SN) midbrain (Fig. S4*A*). However, this finding did not rule out the possibility that the efficacy of the autophagic flux is different between these two neuronal populations. In contrast to our observation in SN neurons (Fig.1 *A* and *B*), injection of high titer of AAV–α-syn vector in the VTA resulted in a sustained autophagic response at 3 wk (Fig. S4*B*). Interestingly, when α-syn overexpression was combined with miR-128–mediated repression of TFEB (Fig. 5 *A* and *B*), the VTA neurons became more vulnerable to α-syn–induced toxicity (Fig. 5 *C*–*F*), but overexpression of α-syn or miR-128 alone did not cause any significant loss of this DA neuron population (Fig. S4). Western blot analysis revealed that this sensitization to α-syn toxicity was linked to increased levels of oligomeric α-syn species (Fig. 5*G*) and p62 (1.9-fold, $n = 5$, $P < 0.01$) (Fig. 5*G*).

Pharmacological Stimulation of TFEB Function Induces a Disease-Modifying Effect. Studies reporting the protective effect of rapamycin in various models of neurodegenerative disease suggest that pharmacological stimulation of the ALP via mTOR inhibition may represent an interesting therapeutic strategy (6, 7, 29–33). In line with previous studies (38, 39), mTOR inhibition may alleviate the repression of TFEB and facilitate its shuttling

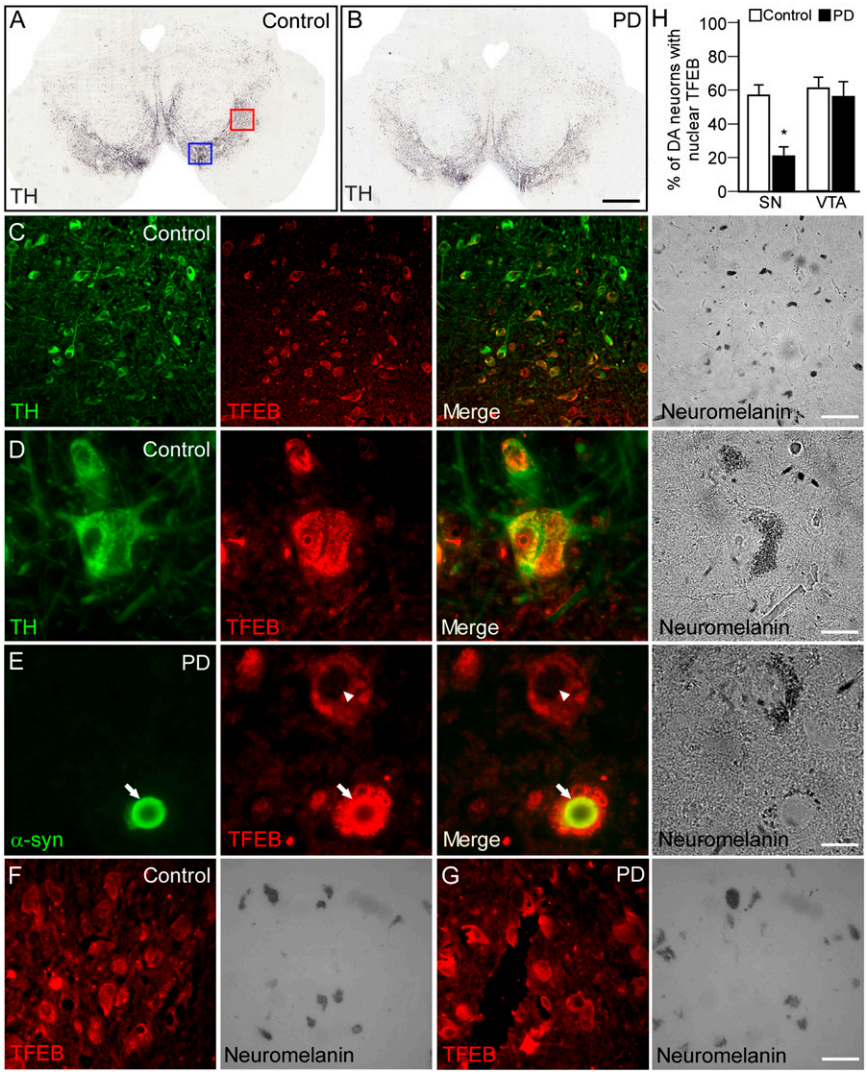

Fig. 2. Changes in TFEB localization in human PD brains. (*A* and *B*) TH immunohistochemistry showing the DA neurons in control and PD human midbrain. Note the reduced density of TH^+ neurons in the PD brain consistent with the clinical diagnostic. Red and blue squares in *A* indicate the regions analyzed to study the expression of TFEB in nigral (shown in *C*–*E*) and VTA neurons (shown in *F* and *G*), respectively. (Scale bar, 500 μm.) (*C* and *D*) Double-immunofluorescence staining of human postmortem midbrain showed that TFEB is well expressed in neuromelanin-containing nigral DA neurons (*C*). (Scale bar, 60 μm.) High-power magnification revealed that TFEB is localized both in the cytoplasmic and nuclear compartments of A9 neurons (*D*). (Scale bar, 12 μm.). (*E*) In PD brains, although the expression level did not seem to be altered, TFEB was not observed in the nuclear compartment and appeared clustered in the cytoplasm (arrowhead). In addition, TFEB colocalized with α-syn in Lewy bodies containing nigral neurons (arrow). Identity of the DA neurons was further confirmed by the expression of neuromelanin (light microscopy). (Scale bar, 12 μm.). Immunofluorescence staining of TFEB from control (*F*) and PD (*G*) human midbrain showing that its pattern of expression is unchanged in VTA DA neurons. (Scale bars, 30 μm.) (*H*) Percentage of nigral and VTA DA neurons presenting TFEB immunoreactivity in the nucleus. A total of 200 neuromelanin-containing cells from five different brains were examined in both the VTA and SN in control and PD human brains.

to the nucleus. Therefore, we tested whether a Food and Drug Administration/European Medicines Agency-approved derivate of rapamycin, CCI-779 (temsirolimus), could afford neuroprotection in a clinically more relevant situation in animals with manifest α-synucleinopthy and ongoing dopaminergic degeneration, as seen at 3 wk after AAV–α-syn injection (Fig. S1). In intact animals, peripheral administration of the drug (three injections, 2 d apart) efficiently inhibited mTOR and S6 phosphorylation and triggered a proautophagic response in the brain, including the ventral midbrain, as seen by the increased levels of ALP markers (Fig. S5). This effect was associated with the nuclear translocation of TFEB (Fig. S5*B*). Interestingly, delayed drug treatment in the AAV–α-syn model, starting 3 wk after vector injection, blocked further progression of the disease. At 8 wk, CCI-779–treated animals did not develop motor impairments in either spontaneous or drug-induced behavior compared with the saline-treated group (Fig. 6 *A*–*C*). Consistent with this finding, significant survival of nigral DA neurons, striatal terminals, and maintenance of striatal DA content was observed in the temsirolimus-treated group compared with controls (Fig. 6 *D*–*H*). Molecular analysis revealed that this disease-modifying effect was mediated by the sustained reduction in phospho-mTOR level, thereby facilitating the nuclear translocation of TFEB (Fig. 6 *K*–*L*). As observed with the gene-transfer approach, survival of nigral DA neurons resulted from the reduced accumulation of toxic oligomeric α-syn (Fig. 6 *I*–*J*).

Discussion

The results highlight TFEB as a central player in the protective response against excessive levels of α-syn in midbrain DA neurons,

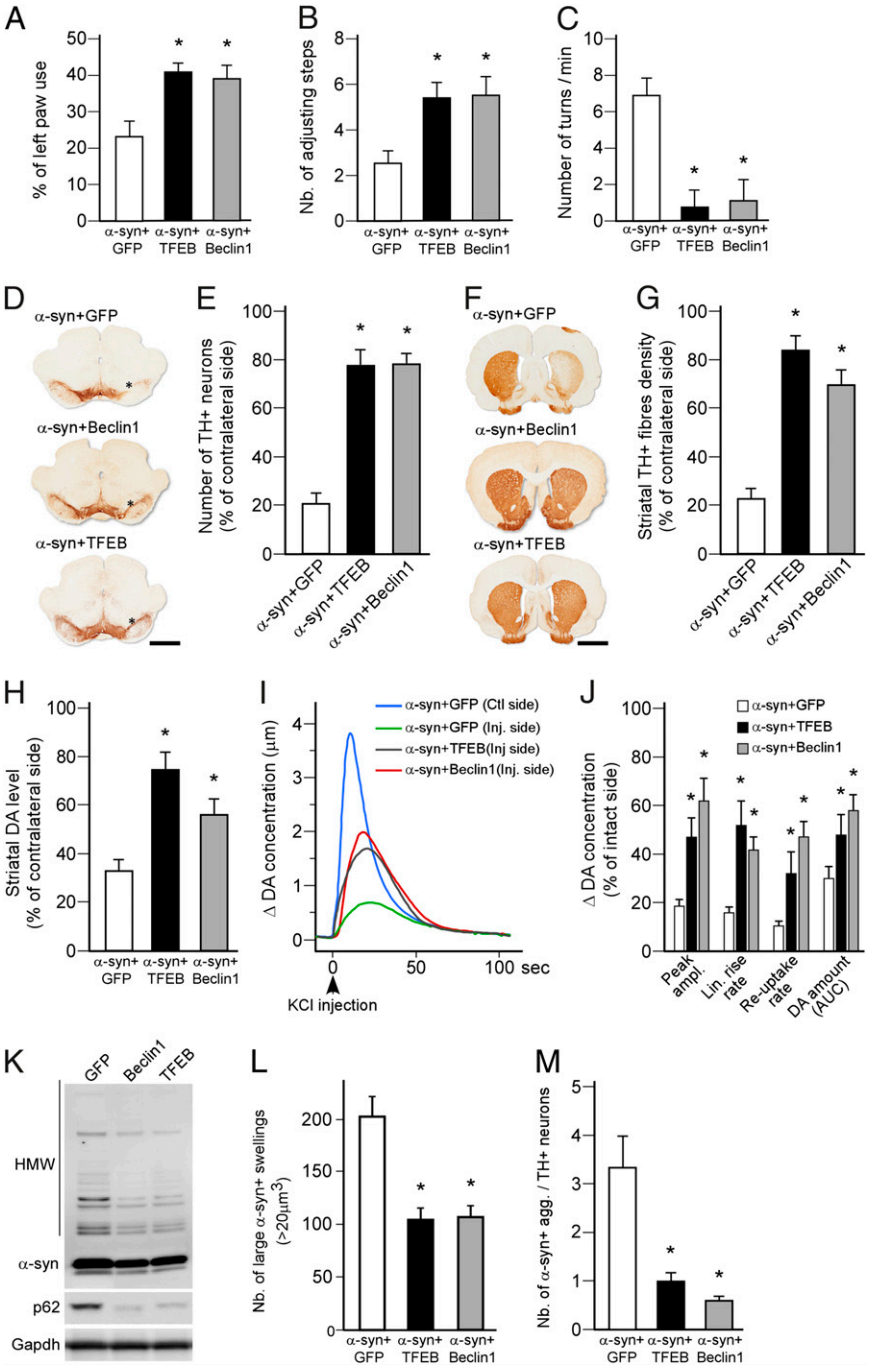

Fig. 3. Gene transfer-mediated stimulation of autophagy protects DA neurons against α-syn toxicity. (*A–C*) Motor function was assessed at 8 wk in rats overexpressing α-syn (high titer: 2.1×10^{12} gc/mL) together with GFP (white bar), TFEB (black bar), or Beclin-1 (gray bar), using the cylinder test (*A*), stepping test (*B*), and amphetamine-induced rotation test (*C*). Overexpression of Beclin-1 and TFEB prevented the development of behavioral deficits in these three tests compared with the GFP group. $*P < 0.05$ compared with AAV-GFP group (one-way ANOVA, Bonferroni post hoc test; $n = 8$ per group). (*D* and *E*) Midbrain sections were stained for TH (*D*) and stereological estimation of the number of TH^+ nigral neurons was performed 8 wk after vector injection (*E*). Counts showed that Beclin-1 and TFEB overexpression afforded robust neuroprotection of nigral DA neurons against α-syn–induced toxicity. $*P < 0.05$ compared with AAV-GFP group (one-way ANOVA, Bonferroni post hoc test; $n = 8$ per group). (Scale bar, 2 mm.) Asterisk indicates injection site. (*F* and *G*) Forebrain sections were stained for TH (*F*) and assessment of striatal TH^+ innervation density was performed by optical densitometry 8 wk after vector injection (*G*). Measurements showed significant survival of striatal TH^+ terminals in the Beclin-1 and TFEB-overexpressing groups compared with GFP control animals. $*P < 0.05$ compared with AAV-GFP group (one-way ANOVA, Bonferroni post hoc test; $n = 8$ per group). (Scale bar, 3 mm.) (*H*) HPLC measurement revealed that striatal DA concentration was significantly higher in rats overexpressing Beclin-1 or TFEB compared with the GFP control group 8 wk after vector injection. $*P < 0.05$ compared with AAV-GFP group (one-way ANOVA, Bonferroni post hoc test; $n = 5$ per group). (*I* and *J*) Representative traces of in vivo real-time chronoamperometry measurements recorded simultaneously from the left (control side) and right (injected side: AAV–α-syn+AAV-GFP or AAV–α-syn+AAV-TFEB and AAV–α-syn+AAV-Beclin-1) striatum after delivery of a KCl pulse (arrow). Quantitative analysis of repeated measurements showed that TFEB or Beclin-1 overexpression significantly preserved DA release (peak amplitude and linear rise rate) and reuptake, as well as the total amount of DA released (AUC, area under the curve) (P). $*P < 0.05$ compared with GFP group (Student *t* test; $n = 5$ per group). (*K*) Western blot analysis showed that Beclin-1 and TFEB-mediated neuroprotection is associated with reduced accumulation of α-syn oligomers (HMW, high molecular weight), and reduced levels of p62 ($n = 5$ per group). (*L*) Computer-based 3D reconstruction of *z*-stacked pictures allowed the detection and quantification of large-sized (>20 μm^3) α-syn$^+$ axonal swellings in the striatum of rats overexpressing α-syn at high titer together with GFP, Beclin-1, or TFEB. Beclin-1 of TFEB overexpression prevented the accumulation of large α-syn$^+$ structures. $*P < 0.05$ compared with GFP group (one-way ANOVA, Bonferroni post hoc test; $n = 8$ per group). (*M*) The load of α-syn was estimated by calculating the ratio of the number of striatal α-syn axonal swellings (Fig. S3 *A–D*) over the number of surviving nigral DA neurons (*F*). Beclin-1 or TFEB overexpression markedly reduced the abundance of α-syn swellings. $*P < 0.05$ compared with AAV-GFP group (one-way ANOVA, Bonferroni post hoc test; $n = 8$ per group).

and provide evidence that stimulation of TFEB function, by gene transfer or pharmacological blockade of mTOR, can efficiently rescue nigral DA neurons from α-syn toxicity.

Under baseline conditions, α-syn will be eliminated by both the proteasome system and the ALP. However, in case of α-syn overload, it has been shown that processing by the ALP becomes the dominant pathway for α-syn removal (12, 13). Here we show that overexpression of human α-syn in nigral DA neurons induces dynamic changes in ALP function that are well correlated with the cytoplasmic retention of a major ALP regulator, TFEB. At an early presymptomatic stage, 10 d after vector injection, when α-syn is well expressed and before any cell death has occurred (42), TFEB was translocated to the nucleus and the expression of lysosomal and autophagic markers was markedly increased. This finding suggests that at this stage TFEB is mobilized to activate the ALP in response to the elevated cytoplasmic levels of α-syn. After 3 wk, when the pathological changes have become prominent and cell death starts to occur (42), TFEB was largely retained in the cytoplasmic fraction and accompanied by a decline in markers of lysosomal function

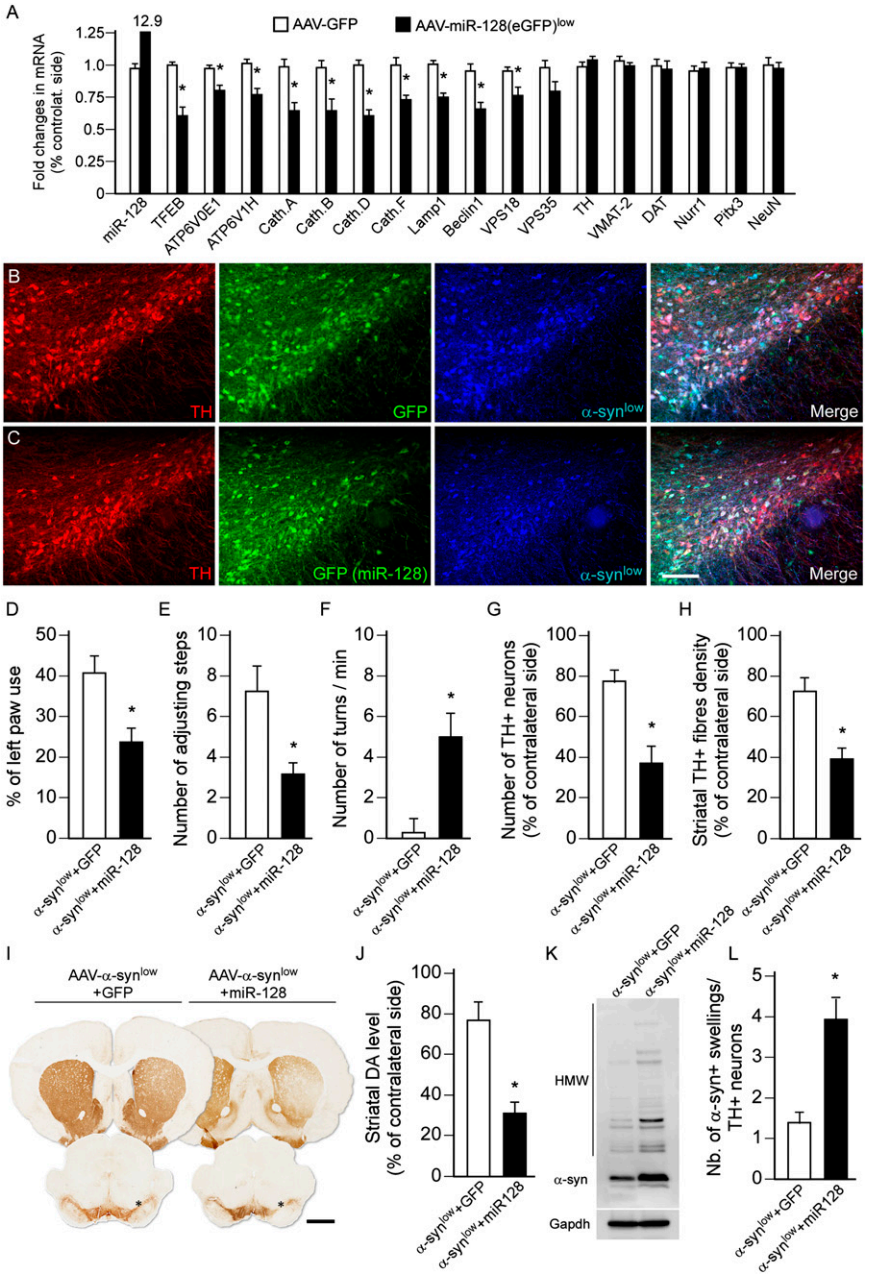

Fig. 4. miR-128-induced inhibition of autophagy aggravates α-syn toxicity. (*A*) Midbrain expression levels of ALP and dopaminergic markers, analyzed by qPCR 3 wk after intranigral injection of AAV-GFP (open bars) or AAV–miR-128 (eGFP) (low titer, 1.2×10^{10} gc/mL, black bars). *$P < 0.05$ compared with GFP group (Student *t* test; $n = 5$ per group). (*B* and *C*) Triple-immunofluorescence staining showing the colocalization of TH (red), GFP (green in B), miR-128 (green, visualized by the GFP reporter in *C*, low titer 1.2×10^{10} gc/mL), and α-syn (low titer: 3.8×10^{11} gc/mL, blue) in nigral DA neurons 3 wk after vector injection. (Scale bar, 100 μm.) (*D–F*) Motor function was assessed at 8 wk in rats overexpressing α-syn at low titer together with GFP or miR-128 using the cylinder test (*D*), stepping test (*E*), and amphetamine-induced rotation test (*F*). miR-128 overexpression (low titer 1.2×10^{10} gc/mL) together with α-syn promoted the development of behavioral deficits on the side controlateral to the vector injection in these three tests compared with the GFP-overexpressing animals. *$P < 0.05$ compared with α-syn+GFP group (Student *t* test; $n = 8$ per group). (*G–I*) Brain sections were stained for TH (*I*) and survival of nigral DA neurons (*G*) and loss of striatal innervation (*H*) was determined at 8 wk by stereological counting and optical densitometry, respectively. Measurements showed that miR-128 overexpression at low titer aggravated α-syn toxicity (low titer: 3.8×10^{11} gc/mL) and triggered a significant loss of nigral TH^+ neurons and striatal TH^+ terminals compared with GFP-overexpressing rats. *$P <$ 0.05 compared with α-syn+GFP group (Student *t* test; $n = 8$ per group). (Scale bar, 1.5 mm.) Asterisk indicates the injection site. (*J*) HPLC measurement showed that striatal DA concentration was significantly lower in rats coexpressing α-syn+miR-128 compared with the GFP controls. *$P < 0.05$ compared with α-syn+GFP group (Student *t* test; $n = 5$ per group). (*K*) Western blot analysis showed that miR-128–mediated inhibition of autophagy enhanced the accumulation of HMW striatal α-syn oligomers ($n = 5$ per group, both vectors delivered at low titer). (*L*) The load of α-syn was estimated by calculating the ratio of the number of striatal α-syn accumulated axonal swellings over the number of surviving nigral TH^+ neurons (*G*). miR-128 overexpression (low titer) significantly increased the burden of α-syn aggregation in these structures. *$P < 0.05$ compared with α-syn+GFP group (Student *t* test; $n = 8$ per group). Data in *J–L* were all obtained at 8-wk survival.

(Lamp-1 and Cathepsin B and D). At this stage, α-syn was colocalized with Beclin-1 and the autophagy substrate p62 in punctate structures, signifying an accumulation of α-syn in autophagosomes and blockade of lysosomal processing, resulting in the progressive accumulation of α-syn oligomers. At lower nontoxic levels of α-syn, the cells survive and the compensatory

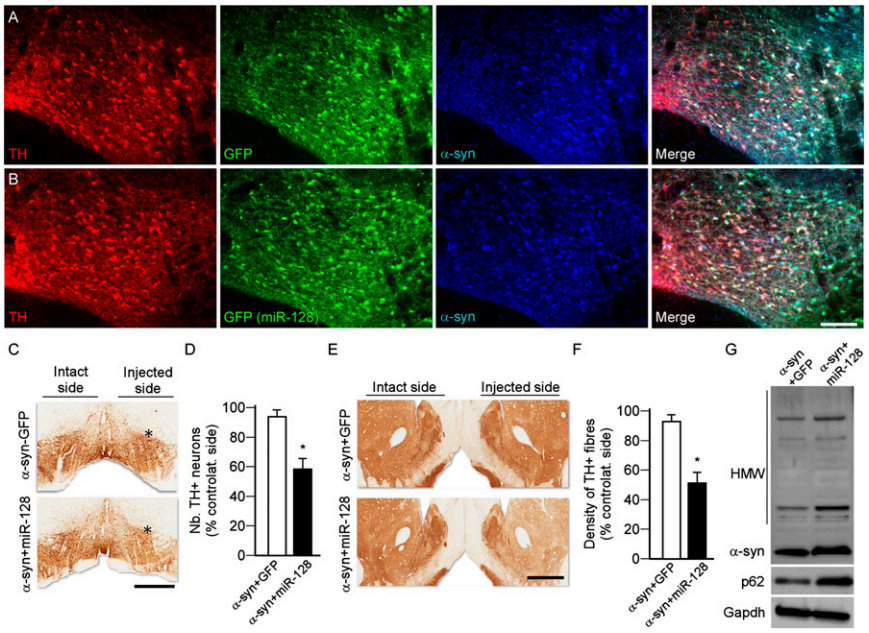

Fig. 5. miR-128-induced knock-down of TFEB renders the A10 neurons more vulnerable to α-syn toxicity. (*A* and *B*) Double-immunofluorescence staining showing the expression of GFP (*A*) and miR-128 (high titer: 6.4×10^{11} gc/mL) (*B*) in green (visualized by the GFP reporter) together with α-syn (high titer: 2.1×10^{12} gc/mL) (in blue) in VTA DA neurons (TH in red), 3 wk after vector injection. (Scale bar, 120 μm.) (*C* and *D*) Midbrain sections from animals overexpressing α-syn at high titer together with GFP or miR-128 (given in high titer) were stained for TH (*C*) and the number of VTA TH^+ neurons was estimated by stereological method (*D*). Co-overexpression of miR-128 made the A10 neurons more sensitive to α-syn–induced toxicity as assessed 8 wk after vector injection. (Scale bar, 500 μm.) $*P < 0.05$ compared with α-syn+GFP group (Student *t* test; $n = 5$ per group). Asterisk indicates the injection site. (*E* and *F*) Forebrain sections were stained for TH (*E*), and TH^+ innervation density was determined by optical densitometry in the nucleus accumbens (*F*). miR-128 overexpression induced a significant loss of TH^+ DA terminals in this structure. (Scale bar, 600 μm.) $*P < 0.05$ compared with α-syn+GFP group (Student *t* test; $n = 5$ per group). (*G*) Western blot analysis showed that coexpression of miR-128, together with α-syn, in VTA neurons promoted the formation of HMW oligomers compared with the α-syn+GFP injected control animals, 8 wk survival ($n = 5$ per group).

up-regulation of the ALP markers was maintained still by 8 wk after vector delivery, consistent with the reduced accumulation of α-syn oligomers. Similar results have been observed in transgenic mice, suggesting that the lack of overt pathological signs in DA neurons in transgenic models may rely on efficient ALP-dependent compensatory mechanisms in response to more modest increases in α-syn expression (6, 52).

The work of Ballabio and colleagues (35, 36) has identified TFEB as a key regulator of ALP activity that is controlled by mTOR signaling (37–39). In vitro and in vivo data suggest that increased expression of this transcription factor can be protective in models of protein misfolding and oxidative stress (7, 35, 40). Similar results have been obtained with forced expression of Beclin-1, which is known to act as an initiator in the formation of the autophagosomes (28). Our results show that overexpression of TFEB (or Beclin-1) is remarkably effective in blocking the development of α-syn–induced pathology and rescuing the nigral DA neurons from degeneration in the AAV–α-syn model. Importantly, the development of behavioral impairments is prevented, and the function at the striatal dopaminergic synapse is well preserved. The exogenous TFEB was located in the nucleus and triggered a sustained increase in markers of ALP activity, such as Lamp-1, Cathepsin B and D, and LC3.

In further support of the central role of TFEB in the handling of toxic α-syn, we used a microRNA approach to down-regulate TFEB and its targets in midbrain DA neurons. Expression of miR-128, identified as a negative regulator of TFEB (35), caused a significant reduction in the expression of both TFEB and its ALP-related targets and resulted in a marked potentiation of α-syn toxicity. The increased toxicity was observed in a situation when α-syn was expressed at a low, nontoxic titer, and was reflected in the development of significant behavioral impairments, accompanied by a marked loss of nigral DA neurons, increased axonal pathology, and increased formation of α-syn oligomers. Moreover, we found that the A10 DA neurons in the VTA, which are remarkably resistant to excess levels of α-syn (51), became vulnerable to α-syn when coexpressed with miR-128. This finding provides support for the idea that the differential vulnerability of nigral and VTA neurons, which is a prominent feature also in human PD (49, 53), may be because of intrinsic differences in the efficiency of lysosomal clearance, and thus the ability of the neurons to resist against toxic concentrations of wild-type or mutated α-syn. It is possible that the effects of mir-128 on α-syn toxicity may also involve other mir-128–related molecular targets important for neuronal survival. Nevertheless, these data provide further support for miR-128 as an endogenous regulator of ALP function, and thus resistance to protein aggregation and toxicity.

The fact that α-syn shares both structural and functional homology with 14-3-3 proteins (46, 47), and the recent finding that phosphorylated TFEB is sequestered in the cytoplasm by 14-3-3 proteins (38), suggests an possible pathogenic mechanism where increased cytoplasmic levels of α-syn could bind to the phosphorylated form of TFEB thus prevents it from getting access to the nucleus. This process, in turn, will result in impaired ALP function and defective clearance of toxic α-syn oligomers. This effect of α-syn is consistent with its chaperone activity described previously (54). Our observations in sections from human postmortem tissue show that TFEB is indeed expressed in human nigral DA neurons and is normally distributed in both the cytoplasm and nucleus. In contrast, in the PD cases TFEB expression in the nuclear compartment was much reduced, providing evidence that this mechanism may be operating also in human PD. Previous observations of postmortem material have shown that

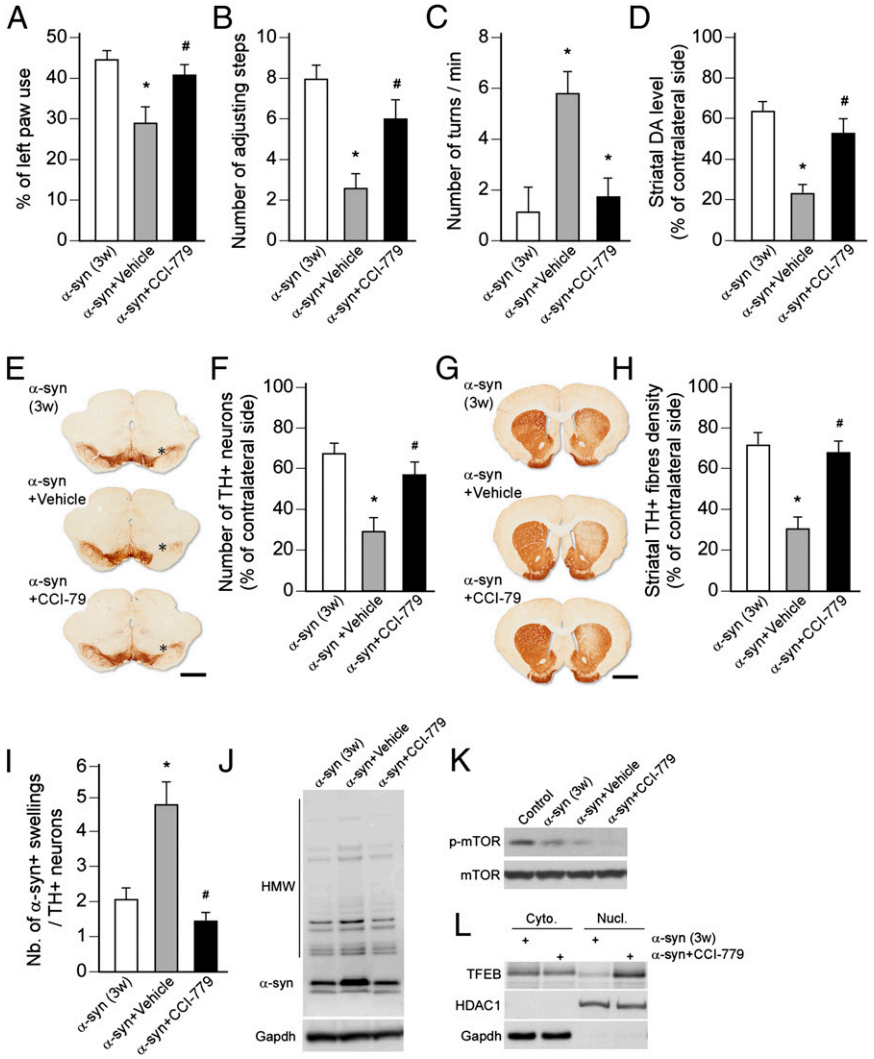

Fig. 6. Delayed mTOR inhibition slows the progression of α-syn–induced neurodegeneration. AAV–α-syn injected rats were treated with CCI-779 (20 mg/kg, three times per week) for 5 wk, starting 3 wk after vector injection. (*A*–*C*) Motor function was assessed at 3 wk in rats overexpressing α-syn (high titer: 2.1×10^{12} gc/mL) (white bar), and at 8 wk in rats treated with CCI-779 (black bar) or vehicle (gray bar) during the last 5 wk, using the cylinder test (*A*), stepping test (*B*), and amphetamine-induced rotation test (*C*). Drug treatment significantly prevented the development of behavioral deficits in these three tests compared with the vehicle-treated animals. $^{*}P < 0.05$ compared with the 3-wk α-syn group; $^{\#}P < 0.05$ compared with α-syn+vehicle group (one-way ANOVA, Bonferroni post hoc test; $n = 8$ per group). (*D*) HPLC measurement revealed that striatal DA concentration was significantly higher in α-syn–overexpressing rats treated with the mTOR inhibitor compared with the vehicle-treated animals. $^{*}P < 0.05$ compared with the 3-wk α-syn group; $^{\#}P < 0.05$ compared with α-syn+vehicle group (one-way ANOVA, Bonferroni post hoc test; $n = 5$ per group). (*E* and *F*) Midbrain sections were stained for TH (*E*) and stereological estimation of the number of TH^+ nigral neurons was performed at 3 wk (i.e., before initiation of treatments) or 8 wk after vector injection (i.e., after 5 wk of treatment) (*F*). Counts showed that delayed CCI-779 treatment, starting at 3 wk, slowed down the neurodegeneration and afforded robust neuroprotection of nigral DA neurons against α-syn–induced toxicity compared with vehicle-treated animals. $^{*}P < 0.05$ compared with the 3-wk α-syn group; $^{\#}P < 0.05$ compared with α-syn+vehicle group (one-way ANOVA, Bonferroni post hoc test; $n = 8$ per group). (Scale bar, 1.2 mm.) Asterisk indicates injection site. (*G* and *H*) Forebrain sections were stained for TH (*G*) and the density of striatal TH^+ innervation was assessed by optical densitometry at 3 or 8 wk after vector injection (*G*). Measurements showed significant survival of striatal TH^+ terminals in the drug-treated groups compared with control animals. $^{*}P < 0.05$ compared with the 3-wk α-syn group; $^{\#}P < 0.05$ compared with α-syn+vehicle group (one-way ANOVA, Bonferroni post hoc test; $n = 8$ per group). (Scale bar, 2 mm.) (*I*) The load of α-syn was estimated by calculating the ratio of the number of striatal α-syn accumulated axonal swellings (Fig. S3 *A*–*D*) over the number of surviving nigral TH^+ neurons (*F*). CCI-779 treatment significantly reduced the abundance of α-syn accumulated swellings. $^{*}P < 0.05$ compared with the 3-wk α-syn group; $^{\#}P < 0.05$ compared with α-syn+vehicle group (one-way ANOVA, Bonferroni post hoc test; $n = 8$ per group). (*J*) Western blot analysis showed that treatment with the mTOR inhibitor reduced the accumulation of HMW striatal α-syn oligomers ($n = 5$ per group). (*K* and *L*) Western blot analysis demonstrated that the neuroprotective effect of CCI-779 was associated with a reduced activation of mTOR (*K*) and alleviation of the sequestration of TFEB in the cytoplasm (*L*). Cellular fractionation was confirmed by the expression of GAPDH and HDAC1 in the cytoplasmic and nuclear fractions, respectively ($n = 5$ per group).

14-3-3 proteins and ALP markers, such as Lamp-1, are present in Lewy Bodies (48, 53, 55). The colocalization of TFEB with α-syn in Lewy Bodies is an intriguing and interesting finding, suggesting that TFEB may be sequestered—and thus inactivated—together with α-syn in the intracellular inclusions. Further experiments will be required to ascertain the ability of α-syn to sequester TFEB in the cytoplasmic compartment in both physiological and pathological conditions.

Recent studies have shown that the nuclear translocation of TFEB is regulated by mTOR, as part of the mTORC1 complex (37–39, 48, 53, 55). Here we show that inhibition of mTOR activity by systemic treatment with the rapamycin analog temsirolimus

was efficient in blocking the development of α-syn–induced pathology in the AAV–α-syn treated rats, including the prevention of DA neurons loss, axonal pathology, and behavioral impairments. In these animals we observed a sustained reduction in phospho-mTOR levels, coupled to an increased nuclear translocation of TFEB and a reduced formation of α-syn oligomers. These data suggest that stimulation of TFEB function through mTOR inhibition may be an efficient tool to block DA neurodegeneration in PD, and also to counteract more widespread α-syn aggregation and pathological changes associated with α-synucleinopathy (6).

In summary, the results highlight TFEB as a key player in the development of α-syn–induced toxicity and PD-like pathogenesis, and identify this transcription factor as an interesting target for neuroprotective or disease-modifying therapies in PD. In the model proposed here, protein clearance by the ALP will initially be activated in response to elevated levels of α-syn, induced by translocation of TFEB to the nucleus. When α-syn reaches toxic levels, more and more of TFEB will be bound to α-syn and sequestered in cytoplasmic inclusions, thus preventing its translocation to the nucleus. Our results show that therapeutic interventions using either genetic strategies to increase TFEB expression, or pharmacological tools aimed to stimulate nuclear translocation of endogenous TFEB (e.g., through inhibition of mTORC1 function) will be effective not only in blocking the development of α-syn–induced toxicity, but also as a disease-modifying intervention to block the progression of the pathology in already affected neurons. Although current mTOR inhibitors, such as rapamycin and temsirolimus, are Food and Drug Administration/European Medicines Agency-approved for use in patients, their pharmacokinetic profile and side effects make them less likely to be useful for long-term use in disease-modifying therapies. Drugs acting further downstream, at the level of TFEB phosphorylation or trafficking within the cell, however, should hold great promise for the development of efficient neuroprotective therapies in patients with PD.

Materials and Methods

Animals. Adult female Sprague–Dawley rats (Charles River), 225–250 g at the time of surgery, were housed two to three per cage with ad libitum access to food and water during a 12-h light/dark cycle. All surgical procedures and treatments were conducted in accordance with guidelines set by the Ethical Committee for the Use of Laboratory Animals in the Lund-Malmö region and the European Ethical Committee (86/609 EEC).

Vector Production. Production of the AAV2/6 vectors was performed as previously described (41). The expression of human wild-type α-syn, GFP, and miR-128 were driven by the human synapsin-1 promoter and enhanced using a woodchuck hepatitis virus posttranscriptional regulatory element (WPRE). A miR-128 overexpression AAV-vector was obtained by PCR-amplification of a 396-bp genomic fragment from mouse DNA encompassing mmu-miR-128-1. This fragment was subsequently cloned in-between the GFP and WPRE sequence in an AAV-Synapsin-GFP-WPRE plasmid (56).

Briefly, transfer plasmids carrying AAV2 inverted terminal repeats coding for a human wild-type α-syn, downstream to a synapsin-1 promoter, were generated. The transfection into HEK 293 cells was carried out using the calcium-phosphate method, and included the packaging plasmids pDP6 encoding AAV6 capsid proteins (57, 58). The cells were treated with a lysis buffer (50 mM Tris, 150 mM NaCl, pH 8.4) and by performing freeze-thaw cycles in dry ice/ethanol bath. The crude lysates were purified first by ultracentrifugation (1.5 h at 350,000 × *g* at 18 °C) in a discontinuous iodixanol gradient and the virus containing fractions were purified with ion-exchange chromatography using FPLC. Genome copy titers were determined by real time quantitative PCR, and the following vector concentrations were used: AAV–α-syn (high concentration): 2.1×10^{12} gc/mL; (low concentration): 3.8×10^{11} gc/mL; AAV–miR-128 (eGFP) (high concentration): 6.4×10^{11} gc/mL; (low concentration): 1.2×10^{10} gc/mL; AAV-TFEB: 2.2×10^{11} gc/mL; AAV–Beclin-1: 5.1×10^{11} gc/mL. An AAV-GFP vector was injected as control at a dilution that matched the number of genome copy per milliliter of the transgene of interest. Throughout the text, figures, and legends, α-syn refers to the high titer and $\alpha\text{-syn}^{low}$ refers to the low titer. Similar annotation applies for the AAV–miR-128 (eGFP) vector.

Surgical Procedures. All surgical procedures in rats were performed under general anesthesia using a 20:1 mixture of fentanylcitrate (Fentanyl) and medetomidin hypochloride (Dormitor) (Apoteksbolaget), injected intraperitoneally.

Vector solutions were injected using a 10-μL Hamilton syringe fitted with a glass capillary (outer diameter of 250 μm). Rats received 3 μL of AAV–α-syn, AAV-GFP, AAV-TFEB, AAV–Beclin-1, or AAV–miR-128 (eGFP) or a 1:1 mixture of AAV–α-syn with one of the other vectors. Infusion was performed at a rate of 0.2 μL/min and the needle was left in place for an additional 3-min period before it was slowly retracted. Injection was carried out unilaterally on the right side, at the following coordinates (flat skull position) (59) for the SN: antero-posterior: −5.3 mm, medio-lateral: −1.7 mm, dorso-ventral: −7.2 mm below dural surface; and for the VTA: antero-posterior: −5.3 mm, medio-lateral: −0.9 mm, dorso-ventral: −7.4 mm below dural surface, calculated relative to bregma according to the stereotaxic atlas of Paxinos and Watson (60).

Drug Treatment. CCI-779 was prepared in ethanol as a stock solution at 50 mg/mL on the day of experiment and diluted it to 20 mg/mL in 0.15 M NaCl, 5% (vol/vol) Tween 20, and 5% (vol/vol) PEG 400 immediately before injection. Rats (n = 8 per group) received intraperitoneal injection of CCI-779 (20 mg/kg) or vehicle three times per week (32). Treatment was initiated 3 wk after AAV–α-syn vector injection and continued over 5 wk. In addition, intact animals (n = 6 per group) were treated with the drug or vehicle during 1 wk (three injections given at day 1, 3 and 5; 20 mg/kg i.p.) and killed 6 h after the last injection, to validate the biological effect of CCI-779.

Study of Postmortem Tissue. Paraffin-embedded midbrain sections from PD patients (n = 5) and age-matched control individuals (n = 5) were provided by the United Kingdom Parkinson's Disease Society Tissue Bank at Imperial College. For histological analysis, sections were first deparaffinised by heating 20 min at 65 °C followed by incubation in xylene and decreasing alcohol concentrations. Antigen retrieval was performed by incubation 20 min in Tris buffer (0.1 M, pH 6.0) and staining procedure was similar as described above. Identification of DA neurons was ascertained by the expression of tyrosine hydroxylase (TH) and the visualization of neuromelanin pigments (Fig. 2).

For each brain, two midbrain sections were analyzed for nuclear/cytoplamic TFEB expression. A minimum of 20 neuromelanin-positive neurons was randomly examined at 40× objective magnification in both the nigral and VTA region (see regions examined in Fig. 2*A*). Data are expressed as percentage of DA neurons with nuclear TFEB.

Cell Counting and Optical Densitometry Analysis. Assessment of the total number of TH^+ neurons in the SN and VTA was made according to the optical fractionator principle, using the mlb Bioscience (Micro Brightfield) StereoInvestigator 10.31 Software. Every fifth section covering the entire extent of these regions was included in the counting procedure. A coefficient of error of <0.10 was accepted. The data are expressed as a percentage of the corresponding area from the noninjected, intact side (n = 8 per group).

Density of TH^+ fibers was measured by densitometry in the striatum at four coronal levels (+1.2, 0.8, 0.00 and −0.4 mm relative to bregma) and in nucleus accumbens at three coronal levels (+2.3, 1.7, and +0.8 mm relative to bregma) using the ImageJ software (v1.32j, National Institutes of Health). The measured values were corrected for nonspecific background staining by subtracting values obtained from the cortex. The data are expressed as a percentage of the corresponding area from the intact side.

Other Experimental Procedures. Additional methods are described in *SI Materials and Methods*.

ACKNOWLEDGMENTS. The authors thank Ulla Jarl, Michael Sparrenius, Jenny Johansson, Elsy Ling, and Björn Anzelius for excellent technical assistance; Prof. Thomas Perlmann for stimulating discussions in the preparation of the manuscript; and Pfizer for providing Temsirolimus. The study was supported by grants from the M. J. Fox Foundation, the Swedish Research Council (Grant 04X-3874 and the Bagadilico program), the Ragnar Söderberg Foundation, the Multipark program, and the Swedish Parkinson's Disease Foundation. The human material (midbrain sections) was provided by the United Kingdom Parkinson's Disease Society Tissue Bank at Imperial College.

1. Levine B, Kroemer G (2008) Autophagy in the pathogenesis of disease. *Cell* 132(1): 27–42.
2. Rubinsztein DC (2006) The roles of intracellular protein-degradation pathways in neurodegeneration. *Nature* 443(7113):780–786.
3. Rubinsztein DC, Mariño G, Kroemer G (2011) Autophagy and aging. *Cell* 146(5): 682–695.
4. Wong E, Cuervo AM (2010) Autophagy gone awry in neurodegenerative diseases. *Nat Neurosci* 13(7):805–811.
5. Chu Y, Dodiya H, Aebischer P, Olanow CW, Kordower JH (2009) Alterations in lysosomal and proteasomal markers in Parkinson's disease: Relationship to alpha-synuclein inclusions. *Neurobiol Dis* 35(3):385–398.
6. Crews L, et al. (2010) Selective molecular alterations in the autophagy pathway in patients with Lewy body disease and in models of alpha-synucleinopathy. *PLoS ONE* 5(2):e9313.
7. Dehay B, et al. (2010) Pathogenic lysosomal depletion in Parkinson's disease. *J Neurosci* 30(37):12535–12544.
8. Lee HJ, Khoshaghideh F, Patel S, Lee SJ (2004) Clearance of alpha-synuclein oligomeric intermediates via the lysosomal degradation pathway. *J Neurosci* 24(8):1888–1896.
9. Vogiatzi T, Xilouri M, Vekrellis K, Stefanis L (2008) Wild type alpha-synuclein is degraded by chaperone-mediated autophagy and macroautophagy in neuronal cells. *J Biol Chem* 283(35):23542–23556.
10. Webb JL, Ravikumar B, Atkins J, Skepper JN, Rubinsztein DC (2003) Alpha-Synuclein is degraded by both autophagy and the proteasome. *J Biol Chem* 278(27):25009–25013.
11. Mak SK, McCormack AL, Manning-Bog AB, Cuervo AM, Di Monte DA (2010) Lysosomal degradation of alpha-synuclein in vivo. *J Biol Chem* 285(18):13621–13629.
12. Xilouri M, Vogiatzi T, Vekrellis K, Park D, Stefanis L (2009) Abberant alpha-synuclein confers toxicity to neurons in part through inhibition of chaperone-mediated autophagy. *PLoS ONE* 4(5):e5515.
13. Cuervo AM, Stefanis L, Fredenburg R, Lansbury PT, Sulzer D (2004) Impaired degradation of mutant alpha-synuclein by chaperone-mediated autophagy. *Science* 305(5688):1292–1295.
14. Ebrahimi-Fakhari D, et al. (2011) Distinct roles in vivo for the ubiquitin-proteasome system and the autophagy-lysosomal pathway in the degradation of α-synuclein. *J Neurosci* 31(41):14508–14520.
15. Martinez-Vicente M, et al. (2008) Dopamine-modified alpha-synuclein blocks chaperone-mediated autophagy. *J Clin Invest* 118(2):777–788.
16. Friedman LG, et al. (2012) Disrupted autophagy leads to dopaminergic axon and dendrite degeneration and promotes presynaptic accumulation of α-synuclein and LRRK2 in the brain. *J Neurosci* 32(22):7585–7593.
17. Hara T, et al. (2006) Suppression of basal autophagy in neural cells causes neurodegenerative disease in mice. *Nature* 441(7095):885–889.
18. Komatsu M, et al. (2006) Loss of autophagy in the central nervous system causes neurodegeneration in mice. *Nature* 441(7095):880–884.
19. Usenovic M, Tresse E, Mazzulli JR, Taylor JP, Krainc D (2012) Deficiency of ATP13A2 leads to lysosomal dysfunction, α-synuclein accumulation, and neurotoxicity. *J Neurosci* 32(12):4240–4246.
20. Mazzulli JR, et al. (2011) Gaucher disease glucocerebrosidase and α-synuclein form a bidirectional pathogenic loop in synucleinopathies. *Cell* 146(1):37–52.
21. Winder-Rhodes SE, et al. (2012) Genetic and pathological links between Parkinson's disease and the lysosomal disorder Sanfilippo syndrome. *Mov Disord* 27(2):312–315.
22. Pang S, Chen D, Zhang A, Qin X, Yan B (2012) Genetic analysis of the LAMP-2 gene promoter in patients with sporadic Parkinson's disease. *Neurosci Lett* 526(1):63–67.
23. Ramirez A, et al. (2006) Hereditary parkinsonism with dementia is caused by mutations in ATP13A2, encoding a lysosomal type 5 P-type ATPase. *Nat Genet* 38(10): 1184–1191.
24. Harris H, Rubinsztein DC (2012) Control of autophagy as a therapy for neurodegenerative disease. *Nat Rev Neurol* 8(2):108–117.
25. Rubinsztein DC, Gestwicki JE, Murphy LO, Klionsky DJ (2007) Potential therapeutic applications of autophagy. *Nat Rev Drug Discov* 6(4):304–312.
26. Nascimento-Ferreira I, et al. (2011) Overexpression of the autophagic Beclin-1 protein clears mutant ataxin-3 and alleviates Machado-Joseph disease. *Brain* 134(Pt 5): 1400–1415.
27. Shibata M, et al. (2006) Regulation of intracellular accumulation of mutant Huntingtin by Beclin 1. *J Biol Chem* 281(20):14474–14485.
28. Spencer B, et al. (2009) Beclin 1 gene transfer activates autophagy and ameliorates the neurodegenerative pathology in alpha-synuclein models of Parkinson's and Lewy body diseases. *J Neurosci* 29(43):13578–13588.
29. Bové J, Martínez-Vicente M, Vila M (2011) Fighting neurodegeneration with rapamycin: Mechanistic insights. *Nat Rev Neurosci* 12(8):437–452.
30. Malagelada C, Jin ZH, Jackson-Lewis V, Przedborski S, Greene LA (2010) Rapamycin protects against neuron death in in vitro and in vivo models of Parkinson's disease. *J Neurosci* 30(3):1166–1175.
31. Menzies FM, et al. (2010) Autophagy induction reduces mutant ataxin-3 levels and toxicity in a mouse model of spinocerebellar ataxia type 3. *Brain* 133(Pt 1):93–104.
32. Ravikumar B, et al. (2004) Inhibition of mTOR induces autophagy and reduces toxicity of polyglutamine expansions in fly and mouse models of Huntington disease. *Nat Genet* 36(6):585–595.
33. Spilman P, et al. (2010) Inhibition of mTOR by rapamycin abolishes cognitive deficits and reduces amyloid-beta levels in a mouse model of Alzheimer's disease. *PLoS ONE* 5(4):e9979.
34. Schaeffer V, et al. (2012) Stimulation of autophagy reduces neurodegeneration in a mouse model of human tauopathy. *Brain* 135(Pt 7):2169–2177.
35. Sardiello M, et al. (2009) A gene network regulating lysosomal biogenesis and function. *Science* 325(5939):473–477.
36. Settembre C, et al. (2011) TFEB links autophagy to lysosomal biogenesis. *Science* 332(6036):1429–1433.
37. Peña-Llopis S, et al. (2011) Regulation of TFEB and V-ATPases by mTORC1. *EMBO J* 30(16):3242–3258.
38. Roczniak-Ferguson A, et al. (2012) The transcription factor TFEB links mTORC1 signaling to transcriptional control of lysosome homeostasis. *Sci Signal* 5(228):ra42.
39. Settembre C, et al. (2012) A lysosome-to-nucleus signalling mechanism senses and regulates the lysosome via mTOR and TFEB. *EMBO J* 31(5):1095–1108.
40. Tsunemi T, et al. (2012) PGC-1alpha rescues Huntington's Disease proteotoxicity by preventing oxidative stress and promoting TFEB function. *Sci Transl Med* 4(142): 142ra197.
41. Decressac M, Mattsson B, Björklund A (2012) Comparison of the behavioural and histological characteristics of the 6-OHDA and α-synuclein rat models of Parkinson's disease. *Exp Neurol* 235(1):306–315.
42. Decressac M, Mattsson B, Lundblad M, Weikop P, Björklund A (2012) Progressive neurodegenerative and behavioural changes induced by AAV-mediated overexpression of α-synuclein in midbrain dopamine neurons. *Neurobiol Dis* 45(3):939–953.
43. Kirik D, et al. (2002) Parkinson-like neurodegeneration induced by targeted overexpression of alpha-synuclein in the nigrostriatal system. *J Neurosci* 22(7):2780–2791.
44. Winner B, et al. (2011) In vivo demonstration that alpha-synuclein oligomers are toxic. *Proc Natl Acad Sci USA* 108(10):4194–4199.
45. Bjørkøy G, et al. (2009) Monitoring autophagic degradation of p62/SQSTM1. *Methods Enzymol* 452:181–197.
46. Ostrerova N, et al. (1999) alpha-Synuclein shares physical and functional homology with 14-3-3 proteins. *J Neurosci* 19(14):5782–5791.
47. Perez RG, et al. (2002) A role for alpha-synuclein in the regulation of dopamine biosynthesis. *J Neurosci* 22(8):3090–3099.
48. Dehay B, et al. (2012) Loss of P-type ATPase ATP13A2/PARK9 function induces general lysosomal deficiency and leads to Parkinson disease neurodegeneration. *Proc Natl Acad Sci USA* 109(24):9611–9616.
49. Hirsch E, Graybiel AM, Agid YA (1988) Melanized dopaminergic neurons are differentially susceptible to degeneration in Parkinson's disease. *Nature* 334(6180): 345–348.
50. Uhl GR, Hedreen JC, Price DL (1985) Parkinson's disease: Loss of neurons from the ventral tegmental area contralateral to therapeutic surgical lesions. *Neurology* 35(8): 1215–1218.
51. Maingay M, Romero-Ramos M, Kirik D (2005) Viral vector mediated overexpression of human alpha-synuclein in the nigrostriatal dopaminergic neurons: A new model for Parkinson's disease. *CNS Spectr* 10(3):235–244.
52. Lin X, et al. (2012) Conditional expression of Parkinson's disease-related mutant α-synuclein in the midbrain dopaminergic neurons causes progressive neurodegeneration and degradation of transcription factor nuclear receptor related 1. *J Neurosci* 32(27): 9248–9264.
53. Ubl A, et al. (2002) 14-3-3 protein is a component of Lewy bodies in Parkinson's disease-mutation analysis and association studies of 14-3-3 eta. *Brain Res Mol Brain Res* 108(1–2):33–39.
54. Souza JM, Giasson BI, Lee VM, Ischiropoulos H (2000) Chaperone-like activity of synucleins. *FEBS Lett* 474(1):116–119.
55. Kawamoto Y, et al. (2002) 14-3-3 proteins in Lewy bodies in Parkinson disease and diffuse Lewy body disease brains. *J Neuropathol Exp Neurol* 61(3):245–253.
56. Åkerblom M, et al. (2012) MicroRNA-124 is a subventricular zone neuronal fate determinant. *J Neurosci* 32(26):8879–8889.
57. Grimm D (2002) Production methods for gene transfer vectors based on adeno-associated virus serotypes. *Methods* 28(2):146–157.
58. Zolotukhin S, et al. (1999) Recombinant adeno-associated virus purification using novel methods improves infectious titer and yield. *Gene Ther* 6(6):973–985.
59. Torres EM, et al. (2011) Increased efficacy of the 6-hydroxydopamine lesion of the median forebrain bundle in small rats, by modification of the stereotaxic coordinates. *J Neurosci Methods* 200(1):29–35.
60. Paxinos G, Watson C (1986) *The Rat Brain in Stereotaxic Coordinates.* (Academic, San Diego).